

## 极紫外高透射率自支撑硅薄膜滤片

李笑然<sup>1,2\*</sup>, 陈逸文<sup>1,2</sup>, 谢模杰<sup>1,2</sup>, 赵娇玲<sup>2,3</sup><sup>1</sup>上海大学微电子学院, 上海 200072;<sup>2</sup>中国科学院上海光学精密机械研究所薄膜光学实验室, 上海 201800;<sup>3</sup>中国科学院上海光学精密机械研究所强激光材料重点实验室, 上海 201800

**摘要** 自支撑薄膜滤片是极紫外波段重要的透射式光学元件。为获得 13.5 nm 极紫外高透射率滤片, 本文选用硅(Si)作为膜层材料, 通过脉冲直流磁控溅射在可溶性衬底沉积厚度为 50 nm 的 Si 单层膜, 并成功制备了自支撑 Si 薄膜滤片样品。利用 X 射线反射、扫描电镜、同步辐射装置等测试手段分别对样品膜厚、形貌以及光学性能进行了表征, 结果表明, 50 nm 厚的 Si 滤片在 13.5 nm 处透射率达到 86.02%。进一步通过检测样品组分, 结合 IMD 软件计算并分析了滤片氧化程度, 解释了其在 12.5~20 nm 波段理论透射率与测量值之间存在差异的原因。该研究成果将极大地拓宽此类高透射率 Si 滤片在极紫外光学工程领域的应用前景。

**关键词** 极紫外波段; 高透射率; 自支撑滤片; 硅; 薄膜; 氧化

**中图分类号** O484 **文献标志码** A

**DOI:** 10.3788/AOS231172

极紫外(EUV)波段一般位于 10~100 nm 之间<sup>[1]</sup>, 该波段具有更小的衍射极限, 将其用作光源时可大大提高光学系统的分辨率<sup>[2]</sup>。目前 EUV 光源产生的方法主要包括同步辐射源<sup>[3]</sup>、激光等离子体<sup>[4]</sup>、自由电子激光等<sup>[5]</sup>, 这些光源在输出时往往会加入透射式滤片, 用于筛选所需波段。EUV 波段几乎被所有材料在很短距离内吸收<sup>[6]</sup>, 为满足使用需求, 滤片的厚度通常须达到百纳米级甚至几十纳米。网格支撑和自支撑为两种滤片常见结构, 其中, 自支撑结构可以保证更大的透光面积及高透射率, 但易破损, 制备难度也更高。国外较早的 EUV 滤片相关研究可追溯至 20 世纪 60 年代, Hunter 等<sup>[7]</sup>初步制备并表征了 Al、In、Ge、Si 等不同材料的滤片; 2008 年, Bibishkin 等<sup>[8]</sup>实现了 50 nm 厚、13 nm 波长处透射率达 76% 的 Zr/Si 周期多层膜自支撑滤片的制备; 2020 年, Jimenez 等<sup>[9]</sup>报道了 100 nm 厚、7.02 nm 处透射率为 60% 的 Nb/Zr 双层膜自支撑滤片。国内, 同济大学团队曾开展百纳米级自支撑滤片的相关工作<sup>[10-11]</sup>; 2022 年, 长春理工大学团队制备了 80 nm 厚、极紫外通带内最高透射率为 53% 的自支撑 Al 滤片<sup>[12]</sup>; 近期, 中国科学院长春光学精密机械与物理研究所也有基于网格支撑结构的 Al 滤片研究<sup>[13]</sup>。

Si 的  $L_{2,3}$  吸收边位于 13 nm<sup>[7]</sup>, 其在 13.4 nm 附近波长具有良好的透射率<sup>[14]</sup>, 因此作为滤片材料之一已被应用于 EUV 光刻领域<sup>[15]</sup>。Si 材料制备的薄膜通常易损<sup>[16]</sup>, 在已报道的相关研究中, 其多是作为间隔层与

金属材料构建成复合膜系<sup>[15]</sup>, 或是附着于镍网形成网格支撑结构<sup>[16]</sup>; 而基于磁控溅射的 Si 单层膜自支撑结构鲜有报道。2009 年, Chkhalo 等<sup>[17]</sup>有关多层膜滤片的退火研究工作中, 仅提及厚度为 120 nm、透射率为 68.7% 的 Si 单层膜参考样品, 但并未对其做深入研究。为了推进高透射率滤片在 EUV 领域的应用, 弥补国内外相关方面的研究不足, 本文设计并成功制备了 50 nm 厚度的“超薄”自支撑 Si 薄膜滤片, 重点表征了其 EUV 波段的光谱性能(13.5 nm 处透射率达到 86.02%), 该结果对此类滤片面向 EUV 先进光刻方向的应用具有重要的推动作用。

本文选用纯度 99.999% 的多晶硅靶, 通过脉冲直流磁控溅射工艺分别在氯化钠(NaCl)可溶性衬底和石英衬底上沉积 50 nm 的 Si 单层膜(NaCl 衬底用于自支撑滤片的制备; 石英衬底用于 X 射线反射测试)。工艺参数如下: 本底真空度优于  $1.2 \times 10^{-4}$  Pa, 溅射功率密度为  $2.6 \text{ W/cm}^2$ , Ar 工作压强为 0.25 Pa。薄膜沉积完成后, 使用去离子水将 NaCl 衬底溶解, 再黏合封装即得到通光孔径为 10 mm、膜厚为 50 nm 的自支撑 Si 滤片样品。由此制备完成的样品如图 1 所示, 其表面平整、无明显褶皱。

分别利用 X 射线反射(XRR)和场发射扫描电镜(FE-SEM)对样品厚度及形貌进行表征。考虑到 Si 薄膜表面在空气中会发生自然氧化<sup>[18]</sup>, 因此, 在 XRR 拟合过程中引入了  $\text{SiO}_2$  氧化层。图 2(a)为石英衬底上

收稿日期: 2023-06-21; 修回日期: 2023-07-22; 录用日期: 2023-08-02; 网络首发日期: 2023-08-15

通信作者: \*w16a2z@163.com

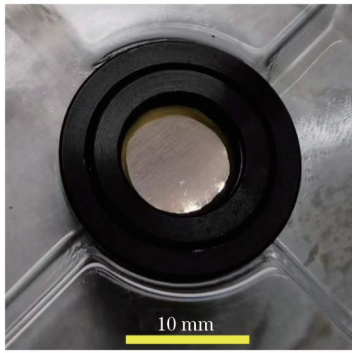


图1 50 nm厚的自支撑Si滤片样品:其表面平整无褶皱

Fig. 1 A sample of 50 nm-thin freestanding Si filter: a flat surface without folding

Si薄膜的中心点附近位置的XRR测试与拟合曲线,拟合结果如表1所示:膜层总厚度为50.8 nm,与设计值

50 nm基本一致;其中SiO<sub>2</sub>层厚度为1.9 nm,表面粗糙度为0.69 nm。进一步,在膜面上选取了13个不同位置且均匀分布的测试点,通过XRR对膜厚的均一性进行了表征,结果汇总于表2中,可见Si薄膜的厚度均一性良好(0.85%的水平)。图2(b)为制得的Si滤片样品的扫描电镜(SEM)图,通过测量,膜层厚度大致为50.26 nm,与XRR拟合结果基本吻合;同时,SEM图显示样品相对致密,未呈现明显多孔结构。

表1 Si薄膜XRR拟合结果

Table 1 XRR fitting results of Si thin film

Layer composition	Thickness of each layer / nm	Roughness / nm
SiO <sub>2</sub> layer	1.9	0.69
Si layer	48.9	0.50

表2 膜厚均一性测试结果

Table 2 Measurement results of film-thickness uniformity

Mean value $\mu$ / nm	Standard deviation $\sigma$ / nm	$M_{ax}$ / nm	$M_{in}$ / nm	$\left(\frac{M_{ax} - M_{in}}{2\mu}\right) / \%$
50.82	0.25	51.25	50.38	0.85

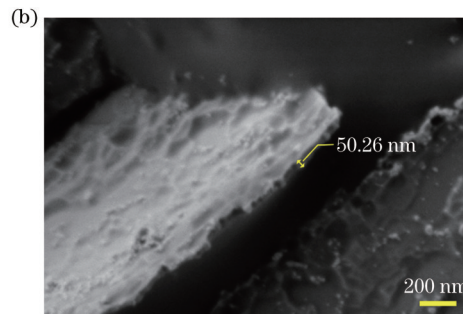
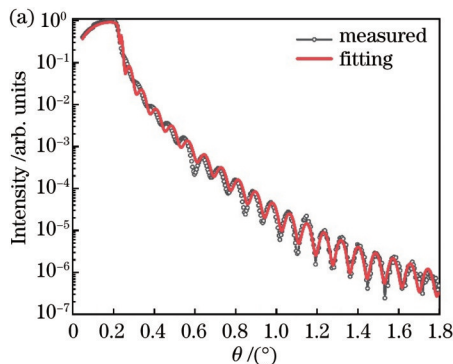


图2 厚度表征结果。(a) Si薄膜XRR测试与拟合曲线;(b) Si滤片断面SEM图

Fig. 2 Measurement results of thickness. (a) XRR measurement and fitting curves of Si thin film; (b) cross-section SEM image of Si filter

采用带有镂空式结构的夹具夹持Si滤片样品,对其EUV波段的光谱性能以及深紫外(DUV)波段的透射率进行了表征,其中,EUV光谱测试是在合肥同步辐射BL08计量站进行的。利用真空紫外光谱仪(ML6500)完成了DUV透射率的测试,其结果显示:Si滤片样品对DUV波段具有良好的滤波阻断特性,其在120~300 nm波段所测得的透射率皆趋于零(最高透射率数值始终小于0.14%的水平)。而在10~20 nm EUV波段, Si滤片样品的透射率测量谱线如图3中“measured”所示,结果表明,在13.5 nm波长处,样品透射率达到86.02%。根据表1中XRR拟合结果,假定滤片上下表面均形成约1.9 nm厚度的SiO<sub>2</sub>层,利用IMD软件<sup>[19]</sup>构建SiO<sub>2</sub>/Si/SiO<sub>2</sub>“三明治”结构模型并展开计算,获得了滤片在10~20 nm波段的理论透射谱线如图3中“cal. 1”所示。对比两条谱线可见,12.5~20 nm波段的透射率测量值整体低于其对应的

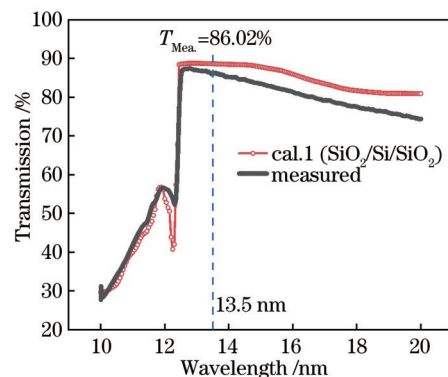


图3 50 nm厚的自支撑Si滤片在10~20 nm波段的透射率测量值及其理论计算值(“cal. 1”),其中13.5 nm处的透射率测量值高达86.02%

Fig. 3 Measured transmission values and theoretical calculation values (“cal. 1”) for 50 nm-thin freestanding Si filter in 10~20 nm band, where a transmission value as high as 86.02% was measured at 13.5 nm

理论值。引起该差别的可能原因如下:一是表面氧化层的成分与厚度假设不精确,导致 IMD 计算出现偏差;二是在溅射沉积过程中,受镀膜设备真空系统漏率的影响,薄膜整体组分、密度等参数不同于纯 Si 膜。为了理解偏差的来源,需进一步分析滤片元素组分等信息。

通过 X 射线光电子能谱仪(XPS)获得了滤片表面 XPS 全谱[图 4(a)]以及深层刻蚀原子百分比分布情况[图 4(b)];由此可见,滤片表层除少量吸附 C 元素外,主要以  $\text{SiO}_x$  的形式存在。由 Si 的刻蚀速率(0.125 nm/s)推算可得,样品单侧表面氧化层  $\text{SiO}_x$  的厚度约为 5 nm(刻蚀时长 40 s)。如图 4(b)所示,随着

刻蚀时间增长,观察到样品深层(刻蚀至 160 s 结束,深度约 20 nm)同样存在着一定程度的“体氧化”现象(氧原子比例始终低于 9.2%),这可能是来自薄膜沉积过程中设备系统漏率或者其他微量污染的影响。结合 XPS 测试结果,对如上 IMD 理论模型进行了相应优化,将“三明治”膜层堆叠由  $\text{SiO}_2/\text{Si}/\text{SiO}_2$  调整为  $\text{SiO}_x/\text{SiO}_y/\text{SiO}_x$ 。表 3 比较了前后两种模型,结果显示,13.5 nm 处的理论透射率由优化前的 88.64% 更新为优化后的 86.20%;而理论透射率与测量值 86.02% 之间的差值( $\Delta T\%$ ),也由此前的 2.62% 降低至 0.18% 左右,吻合情况良好。

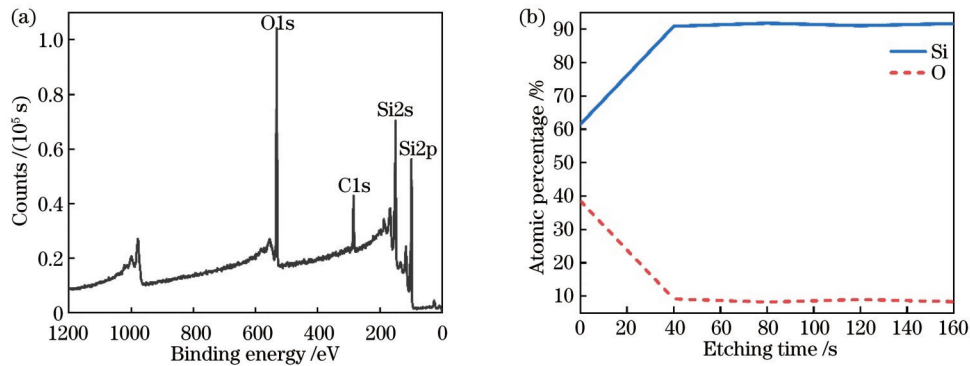


图 4 Si 滤片 XPS 测试结果。(a) 滤片表面 XPS 全谱图;(b) 深层刻蚀原子百分比分布情况

Fig. 4 XPS measurement results of Si filter. (a) XPS full spectra on surface of filter; (b) distribution of atomic percentage during deep etching

表 3 两种 IMD 理论模型对比

Table 3 Comparison of two models used in IMD calculation

Model used	Layer stack	Thickness of oxide layer on one side /nm	Transmission (cal.) at 13.5 nm /%	$\Delta T$ at 13.5 nm /%
“cal. 1”	$\text{SiO}_2/\text{Si}/\text{SiO}_2$	1.9	88.64	2.62
“cal. 2”	$\text{SiO}_x/\text{SiO}_y/\text{SiO}_x$	5.0	86.20	0.18

图 5 为模型优化后计算得到的 Si 滤片 10~20 nm 波段的理论透射率谱线,相较于优化前,此时 12.5~20 nm 波段两条曲线之间的重合度有了明显的改善,二者趋势基本一致,符合预期。该结果说明,滤片样品表面及其深层的氧化程度,均会对其 EUV 波段透射率产生一定程度的削减作用。因此,如何有效降低各类氧化效应,以进一步提升滤片的透光性能,将是今后本方向研究的重点内容。

综上,本文成功制备了厚度为 50 nm 的“超薄”自支撑 Si 薄膜滤片,并重点表征了滤片 EUV 波段的透射光谱(13.5 nm 处透射率高达 86.02%),其同时具备良好的 DUV 波段滤波阻断特性。利用 IMD 建立了滤片“三明治”结构理论模型,结合 XPS 分析证明了 12.5~20 nm 波段透射率测量结果与理论计算曲线的良好吻合,阐明了滤片表面及深层氧化对透射率的影响。本工作所实现的 13.5 nm EUV 高透射率(86.02%) Si 滤片,为此类单层膜滤片拓宽了应用前

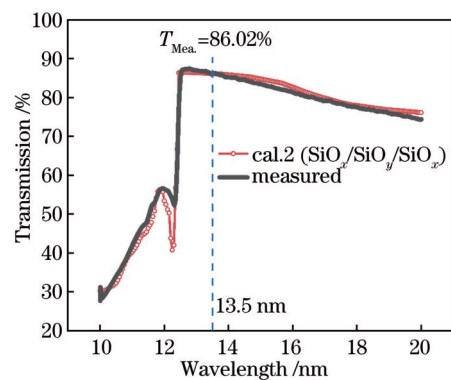


图 5 模型优化后,50 nm 厚的自支撑 Si 滤片在 10~20 nm 波段的透射率测量值及其理论计算值(“cal. 2”)

Fig. 5 Measured transmission values and theoretical calculation values for 50 nm-thin freestanding Si filter in 10-20 nm band after optimization of calculation model (“cal. 2”)

景,例如在 EUV 光刻及其他短波长领域大科学装置中的潜在应用。

致谢 感谢合肥同步辐射国家实验室在光谱测试中提供的大力支持和帮助。

## 参 考 文 献

- [1] Larruquert J I. Optical properties of thin film materials at short wavelengths[M]//Piegarì A, Flory F. Optical thin films and coatings. Amsterdam: Elsevier, 2018: 291-356.
- [2] Torrisi A, Wachulak P W, Bartnik A, et al. Biological applications of short wavelength microscopy based on compact, laser-produced gas-puff plasma source[J]. Applied Sciences, 2020, 10(23): 8338.
- [3] Arp U, Friedman R, Furst M L, et al. SURF III -an improved storage ring for radiometry[J]. Metrologia, 2000, 37(5): 357-360.
- [4] Fujimoto J, Mizoguchi H, Abe T, et al. Laser-produced plasma-based extreme-ultraviolet light source technology for high-volume manufacturing extreme-ultraviolet lithography[J]. Journal of Micro/Nanolithography, MEMS, and MOEMS, 2012, 11(2): 021111.
- [5] Hilbert V, Blinne A, Fuchs S, et al. An extreme ultraviolet Michelson interferometer for experiments at free-electron lasers [J]. Review of Scientific Instruments, 2013, 84(9): 095111.
- [6] Marcos L R D, Larruquert J I, Vidal-Dasilva M, et al. Transmittance and optical constants of Ca films in the 4 - 1000 eV spectral range[J]. Applied Optics, 2015, 54(8): 1910-1917.
- [7] Hunter W R, Angel D W, Tousey R. Thin films and their uses for the extreme ultraviolet[J]. Applied Optics, 1965, 4(8): 891-898.
- [8] Bibishkin M S, Chkhalo N I, Gusev S A, et al. Multilayer Zr/Si filters for EUV lithography and for radiation source metrology [J]. Proceedings of SPIE, 2008, 7025: 702502.
- [9] Jimenez K, Nicolosi P, Juschkin L, et al. Extreme ultraviolet free-standing transmittance filters for high brilliance sources, based on Nb/Zr and Zr/Nb thin films on Si<sub>3</sub>N<sub>4</sub> membranes: design, fabrication, optical and structural characterization[J]. Thin Solid Films, 2020, 695: 137739.
- [10] 伍和云, 吴永刚, 王振华, 等. 自支撑 Zr 膜制备及软 X 射线透  
过性能研究[J]. 光子学报, 2011, 40(1): 1-4.
- [11] 付联效, 吴永刚, 伍和云, 等. 30.4 nm Cr/Al/Cr 自支撑滤光片的研制[J]. 强激光与粒子束, 2009, 21(2): 235-239.
- [12] 唐吉龙, 徐雄伟, 陈田祥, 等. 自支撑 Al 滤光片的制备[J]. 光子学报, 2022, 51(6): 0631001.
- [13] 牛筱茜, 缪鹏飞, 王瀚林, 等. 17.1 nm 极紫外滤光片的制备 [J]. 光学精密工程, 2023, 31(2): 141-149.
- [14] Powell F R, Johnson T A. Filter windows for EUV lithography [J]. Proceedings of SPIE, 2001, 4343: 585-589.
- [15] Chkhalo N I, Drozdov M N, Klunokov E B, et al. Free-standing spectral purity filters for extreme ultraviolet lithography [J]. Journal of Micro/Nanolithography, MEMS, and MOEMS, 2012, 11(2): 021115.
- [16] Labov S, Bowyer S, Steele G. Boron and silicon: filters for the extreme ultraviolet[J]. Applied Optics, 1985, 24(4): 576-578.
- [17] Chkhalo N I, Gusev S A, Drozdov M N, et al. Influence of annealing on the structural and optical properties of thin multilayer EUV filters containing Zr, Mo, and silicides of these metals[J]. Proceedings of SPIE, 2010, 7521: 752105.
- [18] Morita M, Ohmi T, Hasegawa E, et al. Growth of native oxide on a silicon surface[J]. Journal of Applied Physics, 1990, 68(3): 1272-1281.
- [19] Windt D L. IMD—software for modeling the optical properties of multilayer films[J]. Computers in Physics, 1998, 12(4): 360-370.

## Freestanding Silicon Thin-Film Filters with High Transmission in Extreme Ultraviolet Range

Li Xiaoran<sup>1,2\*</sup>, Chen Yiwen<sup>1,2</sup>, Xie Mojie<sup>1,2</sup>, Zhao Jiaoling<sup>2,3</sup>

<sup>1</sup>School of Microelectronics, Shanghai University, Shanghai 200072, China;

<sup>2</sup>Laboratory of Thin Film Optics, Shanghai Institute of Optics and Fine Mechanics, Chinese Academy of Sciences, Shanghai 201800, China;

<sup>3</sup>Key Laboratory of Materials for High Power Laser, Shanghai Institute of Optics and Fine Mechanics, Chinese Academy of Sciences, Shanghai 201800, China

### Abstract

**Objective** Freestanding thin-film filters are important transmissive optical elements for applications in extreme ultraviolet (EUV) bands. Silicon (Si) has the  $L_{2,3}$  absorption edge at the wavelength of 13 nm, providing high transmission at  $\lambda = 13.5$  nm. Therefore, it has been employed as one of the filtering materials in EUV lithography. Previously, Si is mostly adopted as an interlayer to form a multilayer structure with metallic materials, or attached to a nickel mesh to form a grid-supporting structure. However, till now there has been no thorough investigation on self-supporting thin-film filters conducted by sputtering a single-component Si material. To promote the application of Si-based freestanding filters in the EUV field and bridge such a gap in domestic research, we designed and fabricated a 50 nm-thin freestanding Si filter with

high transmission at 13.5 nm.

**Methods** The Si thin film was deposited on soluble or quartz substrates by pulsed direct current (DC) magnetron sputtering, and upon fabrication and gluing for encapsulation, a 50 nm-thickness filter sample with a flat surface is shown in Fig. 1. Then, the film thickness and morphology were characterized by X-ray reflectivity (XRR) and field emission scanning electron microscopy (FE-SEM). The EUV transmission spectrum measurements were performed at the National Synchrotron Radiation Laboratory (NSRL). Furthermore, the difference between the theoretical and measured transmission values of the filter in the 12.5–20 nm band was further analyzed by X-ray photoelectron spectroscopy (XPS) and IMD software calculations.

**Results and Discussions** According to the XRR fitting results shown in Table 1, the measured thickness of the thin film is 50.8 nm with a thin SiO<sub>2</sub> layer of 1.9 nm. Figure 2 (b) presents the cross-section SEM image of the Si filter, indicating the filter thickness around 50.26 nm is consistent with the XRR fitting results. Then, a sandwich model of "SiO<sub>2</sub>/Si/SiO<sub>2</sub>" was built in IMD to calculate the EUV transmission spectra. Figure 3 shows the measured transmission values and theoretical calculation ("cal. 1") values in the 10–20 nm band for the filter sample, demonstrating that the measured transmission value reaches 86.02% at 13.5 nm, with an obvious difference ( $\Delta T\%$ ) between the two curves in the 12.5–20 nm region. To explain this phenomenon, we examined the sample's composition by XPS, as shown in Fig. 4. A 5 nm-thin SiO<sub>x</sub> is the majority compound at the surface, and there is a certain level of "bulk oxidation" according to the deep etching results in Fig. 4 (b). With such optimization of the sandwich model from "SiO<sub>2</sub>/Si/SiO<sub>2</sub>" to "SiO<sub>x</sub>/SiO<sub>y</sub>/SiO<sub>x</sub>" based on these XPS results, in Table 3 and Fig. 5, the  $\Delta T\%$  is decreased from 2.62% to 0.18% and the two curves coincide much better.

**Conclusions** To obtain a highly transmissive EUV filter at 13.5 nm, we prepared a freestanding Si filter (50 nm-thin) with its transmission as high as 86.02% at 13.5 nm, combined with decent suppression in the deep ultraviolet (DUV) range. Meanwhile, the XPS results and the optimized IMD calculation model show that both the surface and bulk oxidation levels of the filters exert a significant influence on its EUV transmission, which is a direction that needs further research efforts. Our results will substantially expand the further applications of such ultra-thin Si filters to areas such as EUV lithography and other large-scale scientific facilities in short wavelengths.

**Key words** extreme ultraviolet (EUV) range; high transmission; freestanding filter; silicon; thin films; oxidation